RESEARCH   **Open Access**

COVID-19 patient serum-derived extracellular vesicles deliver miR-20b-5p induces neutrophil extracellular traps

Yao Liao[1†], Yuheng Liu[1†], Dinghao Li[2†], Shiqi Luo[3,4], Yun Huang[2], Junwei Wu[1], Jin Su[1], Yi Yang[1], Ji Wu[2], Zifeng Zhu[2], Mengxi Yanglan[1], Haiyi Deng[1], Xinyi Wu[1], Junhao Xu[1], Feiyang Cao[1], Chunmei Cai[1], Zhen Li[1], Ruibing Yang[1*], Xiaoyan Deng[1*], Jie Wei[1*] and Lifu Wang[1*]

Abstract

Background Severe cases of COVID-19 are characterized by an excessive presence of neutrophils. Neutrophil extracellular traps (NETs), released by activated neutrophils due to SARS-CoV-2 infection, contribute to lung epithelial cell death and are key drivers in COVID-19-associated immunothrombosis. However, the mechanism underlying NET formation in COVID-19 remain unclear.

Methods Extracellular vesicles (EVs) were isolated from the serum of COVID-19 patients and healthy volunteers, while neutrophils were isolated from blood samples of healthy volunteers. Neutrophils were treated with EVs, and the formation of NETs was observed. To identify the components responsible for the COVID-19-EVs-induced NET formation, we analyzed the expression profiles of microRNA (miRNAs) in COVID-19-EVs. We identified eight highly expressed miRNAs in COVID-19-EVs and explored their potential roles in COVID-19-EVs-mediated NET formation. Additionally, we explored the role of miR-20b-5p in COVID-19-EVs-induced NET formation.

Results In this study, we demonstrate that patients with COVID-19 have a higher concentration of serum EVs (COVID-19-EVs) than healthy controls (Normal-EVs). We also found that COVID-19-EVs are internalized by neutrophils to induced NET formation. Through comprehensive miRNA profiling of COVID-19-EVs versus Normal-EVs, we identified 78 differentially expressed miRNAs, with 27 of these being upregulated and 51 being downregulated. Subsequently, we discovered that COVID-19-EVs that were highly abundant with certain miRNAs promote NET formation.

---

†Yao Liao, Yuheng Liu and Dinghao Li contributed equally to this work.

*Correspondence:
Ruibing Yang
1406740346@qq.com
Xiaoyan Deng
dxyzgy@163.com
Jie Wei
weijiegyey@163.com
Lifu Wang
wanglf@gzhmu.edu.cn

Full list of author information is available at the end of the article

Specifically, miR-20b-5p was found to be the strongest inducer of NET formation of the identified miRNAs. Inhibition of miR-20b-5p resulted in a significant decrease in COVID-19-EVs-mediated induction of NET formation.

Conclusion Herein, we reveal a previously unknown role of COVID-19-EVs in NET formation, which contributes to COVID-19 progression. This study suggests that miR-20b-5p may serve as a potential therapeutic target for COVID-19 treatment.

Keywords COVID-19, Extracellular vesicles, Neutrophil extracellular traps, miRNAs, miR-20b-5p

Background

First reported in December 2019, the severe acute respiratory syndrome coronavirus 2 (SARS-CoV-2), the causative agent of coronavirus disease (COVID-19), led to a pandemic that resulted in a significant number of infections and deaths globally. Common symptoms of COVID-19 include fever, cough, difficulty breathing, fatigue, muscle pain, nausea, vomiting, diarrhea, headache, weakness, runny nose, loss of sense of smell, and loss of taste. COVID-19 can lead to severe illness and death due to various complications such as acute respiratory distress syndrome, pneumonia, stroke-causing blood clots that can cause stroke, liver damage, heart damage, kidney disease, neurological disorders, and sepsis [1]. Severe cases of this disease are characterized by an excessive presence of neutrophils, immature monocytes, and myeloid progenitors during the initial phase of infection [2, 3]. However, we do not yet have a fully comprehensive understanding COVID-19 pathogenesis.

Neutrophils, as the most abundant cells within the innate immune system, play a pivotal role in combating pathogens and exhibit specific antiviral mechanisms [4, 5]. During the initial stages of COVID-19, neutrophils are recruited to the lungs and engage in various pathways to eliminate the invading SARS-CoV-2. However, in patients with COVID-19, excessive activation of neutrophils can result in severe cytokine storms and heightened immune responses [6]. Several clinical studies have demonstrated a correlation between elevated levels of neutrophils in the bloodstream and deteriorating oxygenation in COVID-19 cases [7, 8]. Neutrophils release neutrophil extracellular traps (NETs), which are large extracellular structures composed of decondensed chromatin and adorned with molecules that have immunostimulatory and microbicidal properties. NETs have been observed in the lung tissue surrounding the bronchiolar epithelium, exhibiting individual and spatial variations [9]. In vitro studies have shown that these NETs induce lung epithelial cell death in COVID-19 [10]. To further support these findings, serum samples from individuals with COVID-19 have been shown to stimulate NETs release [11]. Taken together, these studies confirm that NETs are key drivers in COVID-19 immunothrombosis [12].

Extracellular vesicles (EVs), cell-derived nanovesicles that contain different cargos, including proteins, lipids, and nucleic acids, are released by almost every cell in the body and are important mediators of intercellular macromolecule transport. Some EVs cargo can also induce harmful proinflammatory and coagulation effects, leading to tissue damage and thrombosis in many cardiovascular diseases, thereby potentially contributing to the pathology of vascular conditions in COVID-19 [13]. Moreover, platelet- and granulocyte-derived EVs have been shown to be upregulated in patients with COVID-19 [13]. Studies have also shown that platelet-derived EVs mediate COVID-19-associated immunothrombosis [14]. Furthermore, EVs carrying tissue factors are linked to the production of plasma thrombin production and disease severity, with higher plasma thrombin expression in patients with COVID-19 requiring mechanical ventilation [15, 16]. Importantly, EVs provide a unique mode of intercellular communication in which microRNAs (miRNAs) produced and released by one cell are taken up by distant cells, where they can alter the cell state [17].

In this study, we demonstrate that COVID-19 patient serum-derived EVs induce NET formation and we reveal the specific miRNAs responsible for this phenotype, with miR-20b-5p being the strongest inducer.

Methods

Samples and ethics

Human serum and blood samples were obtained from The Second Affiliated Hospital of Guangzhou Medical University. Further, this study was approved by the ethics committee of The Second Affiliated Hospital of Guangzhou Medical University (approval number 2023-hs-17-02). The information on healthy volunteers and COVID-19 patients are detailed in Table 1.

EVs purification

To prepare EVs, serum samples were centrifuged at a low speed (300 ×g for 10 min at 4 ℃) in a 15 mL polypropylene tube, using a swinging bucket rotor centrifuge (Model A-4-44 5804R Refrigerated Centrifuge, Eppendorf, Germany). The resulting supernatants were then centrifuged at 2000 ×g for 10 min at 4 ℃. The supernatants were transferred into a 1.5 mL polypropylene tube (Eppendorf, Germany) using a micropipette, and subsequently centrifuged at 10,000 ×g for 60 min at 4 ℃ using a fixed angle rotor (Angle was 45 degrees, model #3331, D-37520

Table 1 The information on healthy volunteers and COVID-19 patients

Clinical features	Healthy volunteers ($n=25$)	COVID-19 patients ($n=25$)
Age, mean (SD)	55.92 (15.7)	56.2 (14.4)
Gender		
male, no. (%)	10 (40)	15 (60)
female, no. (%)	15 (60)	10 (40)
Leucocytes ($\times 10^9$/L)	6.82 (5.7–8.8)	10.53 (8.2–18.3)
Neutrophil, %	64.4 (58.0-73.4)	87.7 (76.50–92.6)
Postive COVID-19 nucleic acid test, no. (%)	0 (0)	25 (100)

Refrigerated Centrifuge, Thermo Electron Corporation, USA). The resulting supernatants were transferred into a Quick-Seal Centrifuge tube (Beckman Coulter, USA) and centrifuged at 120,000 g for 90 min at 4 °C in an Optima L-100xp tabletop ultracentrifuge (Swinging bucket rotor, model SW40 Ti, Optima L-100xp, Beckman Coulter, USA). The resultant pellet (EVs) was then diluted with phosphate-buffered saline (PBS) and subjected to an additional centrifugation step at 120,000 ×g for 90 min at 4 °C using the same Optima L-100xp tabletop ultracentrifuge (Swinging bucket rotor, model SW40 Ti, Optima L-100xp, Beckman Coulter, USA).

EVs identification
Negative-staining transmission electron microscopy (TEM) was utilized to analyze the EVs. Briefly, EVs were placed on a copper grid and negatively stained with 3% (w/v) aqueous phosphotungstic acid solution for 1 min. Subsequently, the grid was examined using a FEI Tecnai G2 Sprit Twin TEM (FEI, USA). Additionally, the EVs particles were analyzed using Nanoparticle tracking analysis (NTA, NanoSight NS300, Malvern Instruments, United Kingdom). The NanoSight NS300 instrument, equipped with a sCMOS camera, a 488 nm laser (Blue), and NTA 3.3 Dev Build 3.3.30 software, was employed for this analysis, and the number of frames was 749.

Neutrophil isolation
Neutrophils were isolated from patient blood samples using an isolation kit (Beijing Solarbio Science & Technology Co., Ltd, China) following the manufacturer's instructions. Neutrophils were further purified by positive selection for CD11b$^+$Ly6G$^+$ cells by flow cytometry using a BD Influx™ Cell Sorter (BD influx, USA) before culture and incubation in a humidified incubator at 37 °C with 5% CO$_2$.

EVs uptake experiment
To label the EVs, they were incubated with PKH26 (PKH26, Sigma-Aldrich, USA) for 5 min. Subsequently,

1% BSA was added in equal volume to terminate the staining. The solution was transferred to a Quick-Seal Centrifuge tube (Beckman Coulter, USA) and centrifuged at 120,000 g for 90 min at 4 °C, using an Optima L-100xp tabletop ultracentrifuge (Swinging bucket rotor, model SW60 Ti, Optima L-100xp, Beckman Coulter, USA). The PKH26-labeled EVs pellet was diluted with PBS and subjected to another centrifugation process at 120,000 g for 90 min, at 4 °C, using an Optima L-100xp tabletop ultracentrifuge (Swinging bucket rotor, model SW60 Ti, Optima L-100xp, Beckman Coulter, USA). Following this, neutrophils were incubated with PKH26-labeled EVs for an hour, and EVs internalization was assessed using confocal analysis. Actin labeling was done using Alexa Fluor Phalloidin-FITC (CST, USA), while DAPI was utilized to detect nuclei.

Immunofluorescence analysis
Neutrophils were cultured on coverslips and treated with the following treatments and times: Normal-EVs (20 μg/mL), 24 h; COVID-19-EVs (20 μg/mL), 24 h; Epstein-Barr virus infection patients serum EVs (EB-EVs), Serum EVs from patients with influenza A (Influenza A-EVs), Normal-EVs-Free (20 μg/mL), 24 h; COVID-19-EVs-Free (20 μg/mL), 24 h; NC mimic (a universal negative control for the study of miRNA mimic, 50 nM), 24 h; miR-20b-5p mimic (50 nM), 24 h; 9-37654 mimic (50 nM), 24 h; 2-18444 mimic (50 nM), 24 h; 11-5823 mimic (50 nM), 24 h; 18-16034 mimic (50 nM), 24 h; 11-5766 mimic (50 nM), 24 h; 1-1765 mimic (50 nM), 24 h; miR-4271 mimic (50 nM), 24 h; Inhibitor NC (50 nM), 24 h; and miR-20b-5p inhibitor (50 nM), 24 h. Phorbol-12-my-ristate-13-acetate (150 nM [PMA]; NETs-inducer) was added 5 h prior to cell collection to stimulate NET formation. After treatment, neutrophils were fixed in 4% paraformaldehyde and permeabilized with 0.2% Triton X-100 in phosphate buffered saline (PBS). Then the cells were blocked with 2% BSA for 30 min at room temperature. Subsequently, the cells were incubated with anti-H3Cit (1:400; CST, USA), anti-MPO (Myeloperoxidase) (1:100; Abcam, UK) antibodies, and SYTOX Green (0.03μM; ThermoFisher Scientific, USA) overnight at 4 °C. The cells were then incubated with the indicated Alexa-Fluor-conjugated secondary antibodies. DAPI was used for nuclei detection. All steps were followed by three 5-minute washes in PBS. The sections were visualized using a Laser Scanning Confocal Microscope LSM 800 (Zeiss, Germany). The NETs were determined as the percentage of the positive H3cit signal in each field of view in the overall cell slides [18]. For NETs quantification, NETs were counted in at least 10 fields per slide and 6 slides per group.

Scanning electron microscopy

As mentioned above, neutrophils were cultured on coverslips and treated with PMA, EVs, and miRNA mimic. To prepare the samples for observation, the neutrophils were fixed overnight in a solution of 2.5% glutaraldehyde. Subsequently, the samples were washed with PBS and dehydrated using gradient ethanol. This process was followed by ethanol exchange with acetone and isoamyl acetate. Finally, the samples were critically dried and coated with gold using an ion coater (E-102, Hitachi). The prepared samples were then examined and photographed using a FEI Quanta 200 scanning electron microscope.

Small RNA sequencing and analysis

Small RNAs were sequenced and analyzed as previously described [19]. Initially, EVs were isolated, and total RNA was extracted to serve as the substrate for small RNA library creation. The library preparations were then subjected to cluster generation and sequenced utilizing the Illumina Hiseq 2500 platform (Illumina, USA). This generated a dataset that underwent preliminary analyses consisting of quality control analysis, comparative analysis, functional annotation of target genes, quantification of miRNA expression levels, as well as GO and KEGG enrichment analysis, using software Bowtie (v1.0.0), miRDeep2 (v2.0.5), IDEG6, edgeR (v3.12.1), miRanda (v3.3a), blast (v2.2.26), and topGO (v2.18.0).

Statistical analysis

Results are presented as mean ± SD values. The data of two groups were analyzed using unpaired two-sample *t*-test. Multiple comparisons between more than two groups were analyzed by one-way ANOVA with Dunnett's multiple comparison test. P-values < 0.05 were considered statistically significant. Immunofluorescence and SEM analyses of NETs were quantified using Image J software. GraphPad Prism 8.0 was used to perform all statistical analyses.

Results

Characterization of COVID-19 patient-derived serum EVs and neutrophil internalization

Patient serum-derived EVs samples were first analyzed by NTA and negative-staining TEM. NTA showed that EVs from healthy volunteers (Normal-EVs) were 97 nm in size compared to 90 nm for COVID-19 patient-derived EVs (COVID-19-EVs). Further, we found that there was an increased abundance of circulating EVs in the patients with COVID-19 (Fig. 1A). Negative-staining TEM analysis of EVs revealed a typical size of 30–200 nm with a characteristic cup-shaped morphology (Fig. 1B). These results confirmed that the isolated circulating nanoparticles were indeed EVs.

Neutrophils serve as the initial responders that migrate to sites of inflammation to combat infections and initiate the immune response. In COVID-19, the primary viral infection of pulmonary type-II pneumocytes trigger an inflammatory response, including the release of inducers of neutrophil colony formation (GM-CSF 2 and 3) and CXC cytokines (such as CXCL8/IL-8), which are potent chemoattractants for neutrophils [20]. This response, combined with the relatively weak production of type I interferons (IFN), leads to the rapid recruitment and activation of neutrophils [20]. To determine the functional impact of EVs on neutrophils, we investigated whether neutrophils could internalize COVID-19-EVs. Interestingly, our findings demonstrated that neutrophils are capable of internalizing COVID-19-EVs (Fig. 1C).

EVs derived from COVID-19 patients induced the formation of NETs

NETs contribute to immunothrombosis in COVID-19 acute respiratory distress syndrome [12, 21]. To investigate the impact of COVID-19-EVs on NETs following neutrophil internalization, neutrophils were isolated from healthy donor blood samples and treated with COVID-19 EVs. Immunofluorescence staining using SYTOX Green, a DNA dye that cannot cross the plasma membrane [22], revealed fibrous structures of extracellular DNA co-localizing with H3cit (NETs) in neutrophils treated with COVID-19-EVs instead of Normal-EVs (Fig. 2A). Additionally, we used PMA as a positive control for NETs induction and observed that COVID-19-EVs enhanced PMA-induced NET formation (Fig. 2B). Moreover, we evaluated the impact of EB-EVs, Influenza A-EVs, and COVID-19-EVs on NET formation. Our results showed that all three types of EVs could induce NET formation and enhanced PMA-induced NET formation, but COVID-19-EVs exhibited a significantly stronger effect (Fig. S1). We also evaluated NETs using H3cit and MPO co-staining to further explore the effect of COVID-19-EVs. Here, we found that COVID-19-EVs (but not Normal-EVs) significantly induced NET formation (Fig. 2C, D). Scanning electron microscopy (SEM) also revealed that COVID-19-EVs notably induced NET formation (Fig. 2E, F). Additionally, compared to the Normal + PMA group, COVID-19-EVs (but not Normal-EVs) promoted PMA-induced NET formation (Fig. 2G, H). Similarly, we further confirmed that COVID-19-EVs can promote the formation of NETs induced by PMA using scanning electron microscopy (Fig. 2I, J). Moreover, we sought to understand whether the stimulatory effect of COVID-19-EVs on NETs differs from the sera of patients with COVID-19. Thus, neutrophils were treated with EVs-depleted COVID-19 patient serum (COVID-19-EVs-Free). Interestingly, COVID-19 EVs-Free samples also induced NET formation, but with a significantly
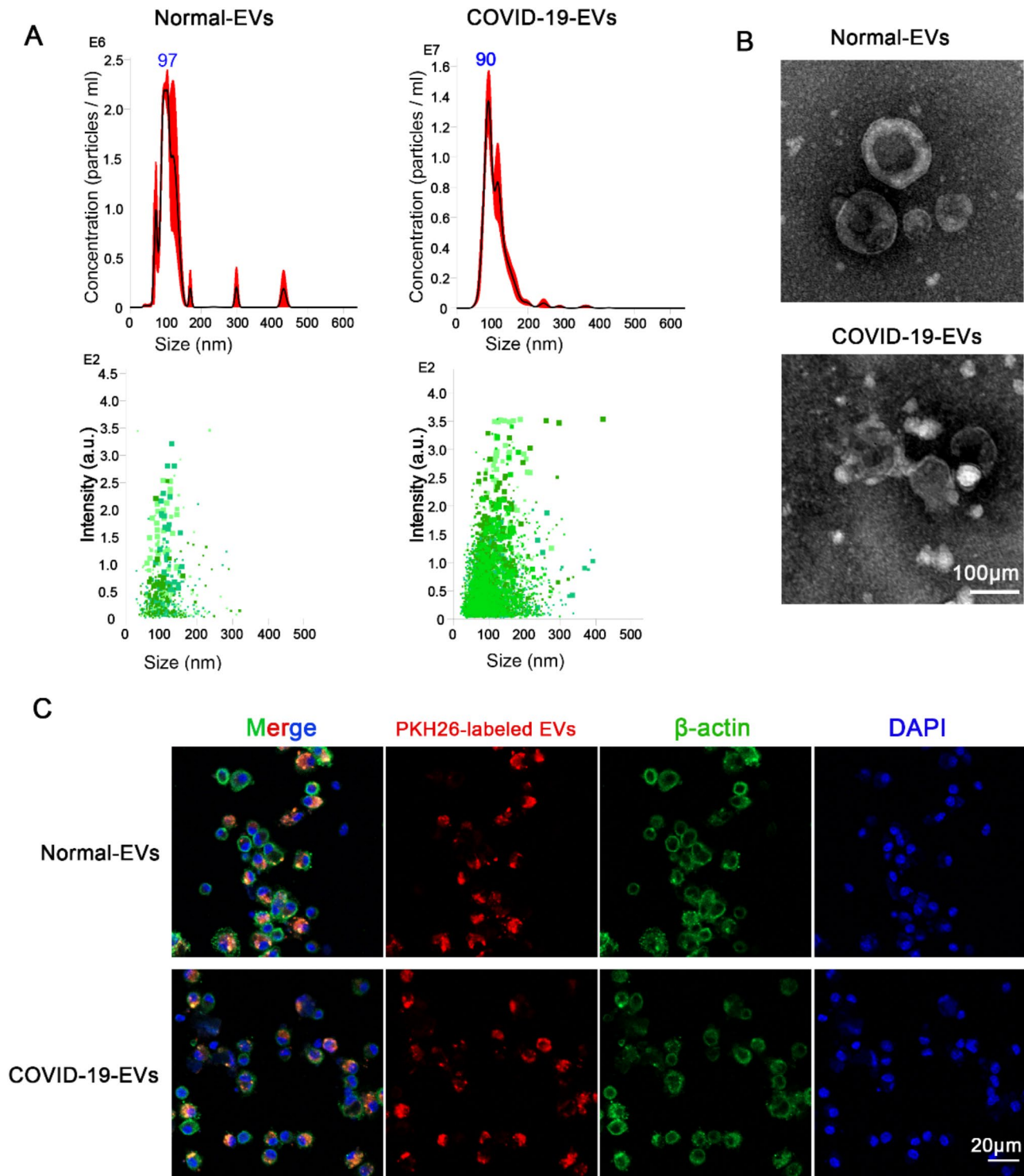
Fig. 1 Characterization of COVID-19 patient serum-derived EVs and neutrophil internalization. **A** EVs derived from serum of healthy volunteers (Normal-EVs) and EVs derived from serum of COVID-19 patients (COVID-19-EVs) were purified by differential centrifugation and analyzed by nanoparticle tracking analysis (NTA). **B** EVs particles were investigated using negative-staining transmission electron microscopy. **C** Neutrophils were incubated with PKH26-labeled EVs for an hour, and EVs internalization was examined using laser scanning confocal microscopy
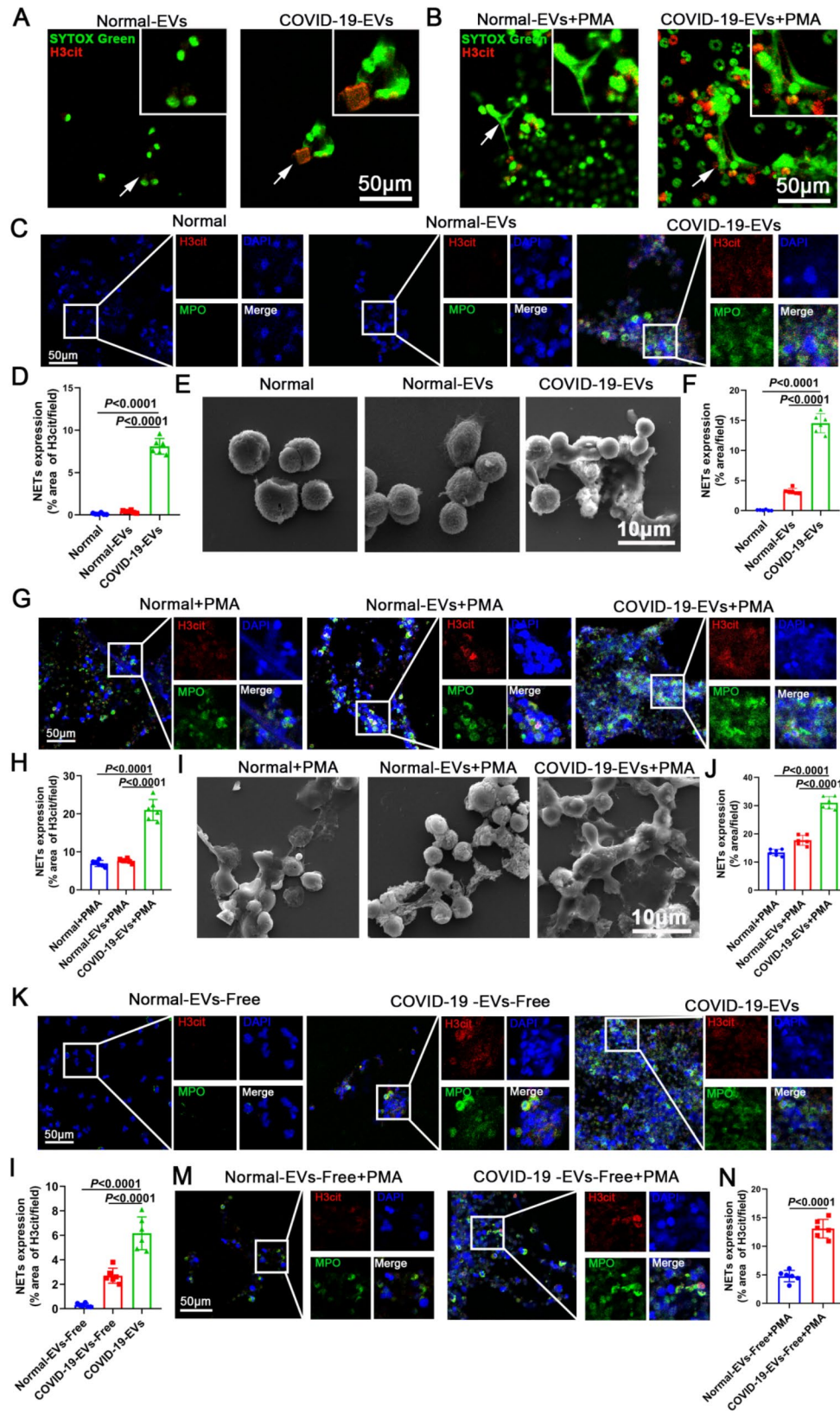
Fig. 2 (See legend on next page.)

(See figure on previous page.)

Fig. 2 EVs derived from COVID-19 patients induced the formation of NETs. **A**-**B** Neutrophils were treated with Normal-EVs, COVID-19-EVs, and phorbol-12-myristate-13-acetate (PMA), and neutrophil extracellular traps (NETs) were detected based on SYTOX Green and H3cit co-localization. **C-F** Neutrophils were treated with Normal-EVs and COVID-19-EVs, NETs were observed using immunofluorescence (IF, NETs were detected based on H3cit and MPO co-localization) and scanning electron microscopy (SEM) (**C** and **E**) and were quantified (**D** and **F**). **G-J** Neutrophils were treated with PMA, Normal-EVs + PMA, and COVID-19-EVs + PMA, NETs were observed using IF and SEM (**G** and **I**) and were quantified (**H** and **J**). **K-L** Neutrophils were treated with Normal-EVs-Free, COVID-19-EVs-Free, and COVID-19-EVs, NETs were observed using IF (**K**) and were quantified (**L**). **M-N** Neutrophils were treated with PMA + Normal-EVs-Free and PMA + COVID-19-EVs-Free, NETs were observed using IF (**M**) and were quantified (**N**). IF was quantified based on area the of H3cit, and SEM was quantified based on the area of NETs. Differences were analyzed using one-way ANOVA with Dunnett's multiple comparison test (**D**, **F**, **H**, **J** and **I**) and unpaired two-sample *t*-test (**N**)

weaker effect compared to COVID-19-EVs (Fig. 2K, L). Furthermore, COVID-19-EVs-Free promoted PMA-induced NET formation (Fig. 2M, N). Taken together, these results suggest that COVID-19-EVs induce NET formation.

Characterization of COVID-19 EVs-derived miRNAs

Within the various EVs cargo components, miRNAs play major roles in regulating gene expression [23]. To identify the components responsible for the COVID-19-EVs-induced formation of NETs, we analyzed the expression profiles of miRNAs in COVID-19-EVs. Through comparative assessments of the global miRNA expression profiles between the COVID-19-EVs and Normal-EVs groups, we found that 78 miRNAs (27 up-regulated and 51 down-regulated) showed significant differential expression (Fig. 3A, B; Table S1). These 78 differentially expressed miRNAs are represented as heatmaps in Fig. 3C. GO analysis showed that these miRNAs were associated with various cellular processes and organelles, including dendrite membranes, AMPA glutamate receptor complexes, responses to platelet-derived growth factor, the Fc receptor mediated stimulatory signaling pathway, and the interleukin-1-mediated signaling pathway (Fig. 3D). AMPA glutamate receptors contribute to inflammation, degeneration, and pain-related behavior in the inflammatory stages of arthritis [24]. Importantly, platelet-derived EVs promote NET formation during septic shock [25]. Further, neutrophils express Fc-receptors to aid recognition of invading pathogens and the inflammatory environment [26]. Interleukin-1 (IL-1) has also been shown to induce NET formation [27]. These findings suggest that these differentially expressed miRNAs are involved in the COVID-19 pathogenesis and NET formation in patients with COVID-19. Furthermore, KEGG analysis was used to identify potential biological pathways related to the identified differentially expressed miRNAs. Our data revealed that these different miRNAs are mainly associated with the MAPK- and cAMP signaling pathways (Fig. 3E). Activation of the MAPK signaling pathway has previously been shown to promote NET formation [28]. Interestingly, Prostaglandin E2 (PGE2) treatment has been shown to limit neutrophil NETosis in a cAMP- and protein kinase A-dependent manner [29]. Therefore, our KEGG analysis results further support our

hypothesis that the differentially expressed miRNAs are implicated in NET formation.

Highly abundant COVID-19 patient serum-derived EVs carry specific miRNAs that are implicated in NET formation

We compared the differences of miRNA expression profiles in COVID-19-EVs and Normal-EVs. We identified eight miRNAs with high expression in COVID-19-EVs, which were selected based on their fold changes (> 180). These miRNAs included 9_37654, 2_18444, 11_5823, 18_16034, 11_5766, miR-20b-5p, 1_1765, miR-4271 (Table 2). We then explored the potential roles of these eight miRNAs in COVID-19-EVs-mediated induction of NET formation using immunofluorescence and SEM. Interestingly, our findings indicate that all of the eight identified miRNAs have the ability to induce NET formation (Fig. 4A-D). Of crucially, we noted the significant stimulatory effect of miR-20b-5p on NET formation (Fig. 4A-D). Furthermore, miR-20b-5p was also shown to significantly promote PMA-induced NET formation (Fig. 4A-D). Collectively, our findings suggest that highly abundant COVID-19 patient serum-derived EVs carry specific miRNAs that are associated with NET formation. Specifically, miR-20b-5p appears to have the strongest induction effect among the identified miRNAs.

COVID-19 patient serum-derived EVs-mediated NET formation is significantly downregulated following miR-20b-5p inhibition

To assess the role of miR-20b-5p in COVID-19 patient serum-derived EVs induction of NET formation, we treated neutrophils with a miR-20b-5p inhibitor (chemically modified mature miR-20b-5p complementary single chain) to reduce miR-20b-5p levels in COVID-19-EVs. As expected, COVID-19-EVs-mediated induction of NET formation decreased significantly following inhibition of miR-20b-5p (Fig. 5A, B). Similarly, following miR-20b-5p inhibition, the promoting effect of COVID-19-EVs on PMA-induced NET formation also decreased significantly (Fig. 5C, D). Together, these results suggest that miR-20b-5p plays an important role in the formation of NETs induced by COVID-19-EVs.
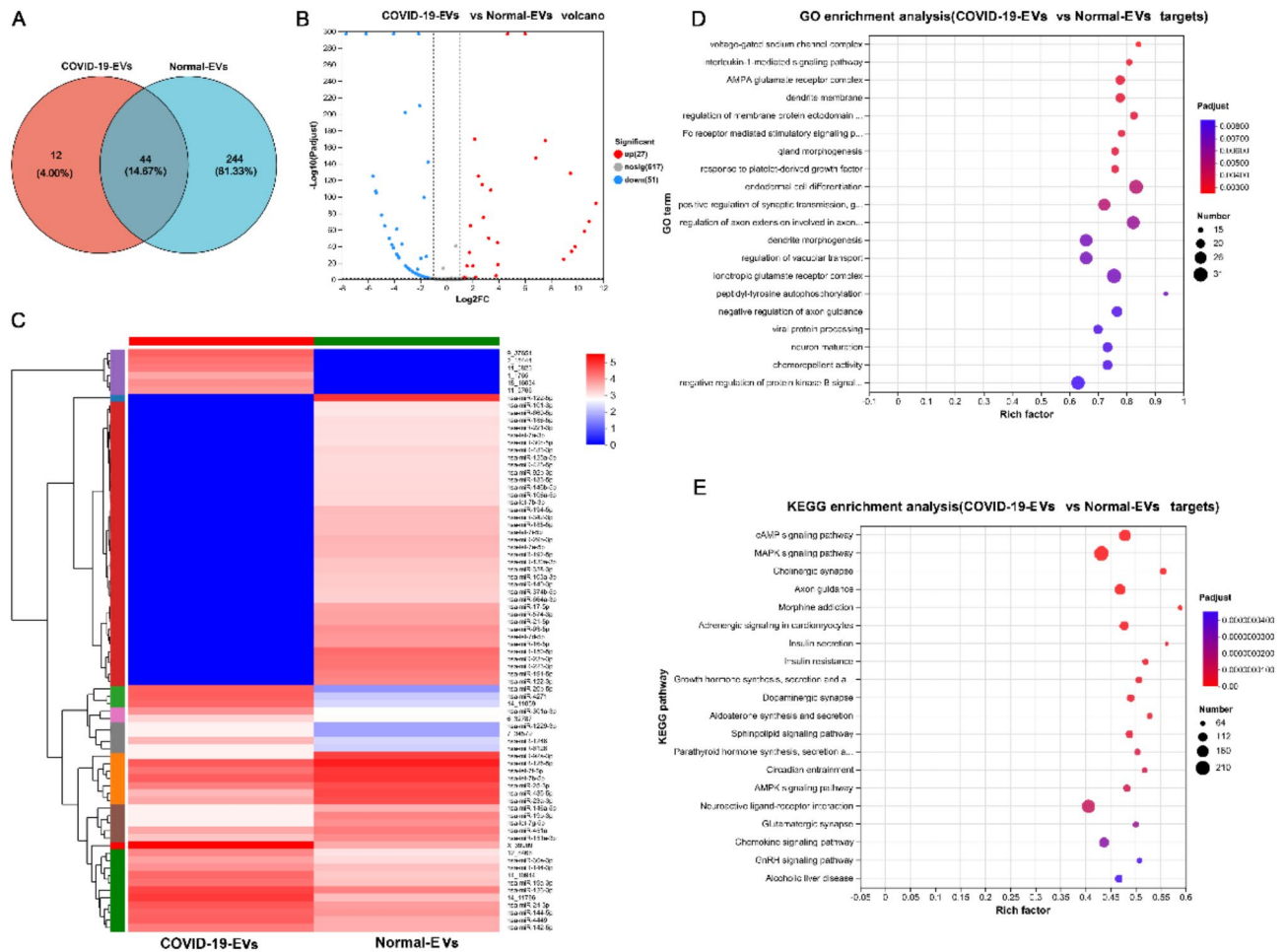
Fig. 3 Characterization of COVID-19 EV-derived miRNAs. **A** Venn diagram showing the microRNAs (miRNAs) that were unique to each group and shared among the two groups. **B** Volcano diagrams highlight 78 miRNAs (27 up-regulated and 51 down-regulated) that exhibit significant differential expression between the COVID-19-EVs and Normal-EVs groups. **C** Heatmaps represent the expression patterns of the 78 differentially expressed miRNAs. **D** GO enrichment analysis is performed to identify functional annotations associated with the differentially expressed miRNAs. **E** KEGG enrichment analysis is conducted to reveal the pathways influenced by the differentially expressed miRNAs

Table 2 The top eight differentially-expressed miRNAs (COVID-19-EVs / Normal-EVs)

NO.	miRNA name	FC	Log2 FC	*P* value	Sequence
1	9_37654	2760.943	11.43094561	7.36E-94	CCCUCUUGGAUAGUCUAUUUCU
2	2_18444	1924.294	10.91011345	7.92E-72	GGGGAGAGGGCGCGGGCGCCGAGU
3	11_5823	1505.969	10.55647649	8.36E-60	GGGGGAGGGGUGGGGAGAGAGAAGG
4	18_16034	920.314	9.845983109	3.09E-41	GUCCCCAGUUACAGAGCUGC
5	11_5766	752.985	9.556476492	2.16E-35	GGCCAGGUGGGCGGGCAGC
6	miR-20b-5p	711.152	9.474014332	3.56E-130	CAAAGUGCUCAUAGUGCAGGUAG
7	1_1765	501.99	8.971513991	6.18E-26	AGGGAAGAAAGGAAGAGGAGGGG
8	miR-4271	188.246	7.556476492	5.71E-170	CAAAGUGCUCAUAGUGCAGGUAG

Discussion

Our results showed that COVID-19 patient serum-derived EVs are internalized by neutrophils leading to NET formation. By examining the expression profiles of miRNAs in these EVs, we also revealed COVID-19-specific EVs carrying specific miRNAs that are associated with stimulation of NET formation. Notably, miR-20b-5p exhibited the most potent stimulatory effect (Fig. 6).

EVs affect the process of virus infection by regulating gene expression as well as the immune status of the body. The composition of serum-derived EVs from patients with COVID-19 is associated with disease severity. Studies have reported an increase in the levels of circulating
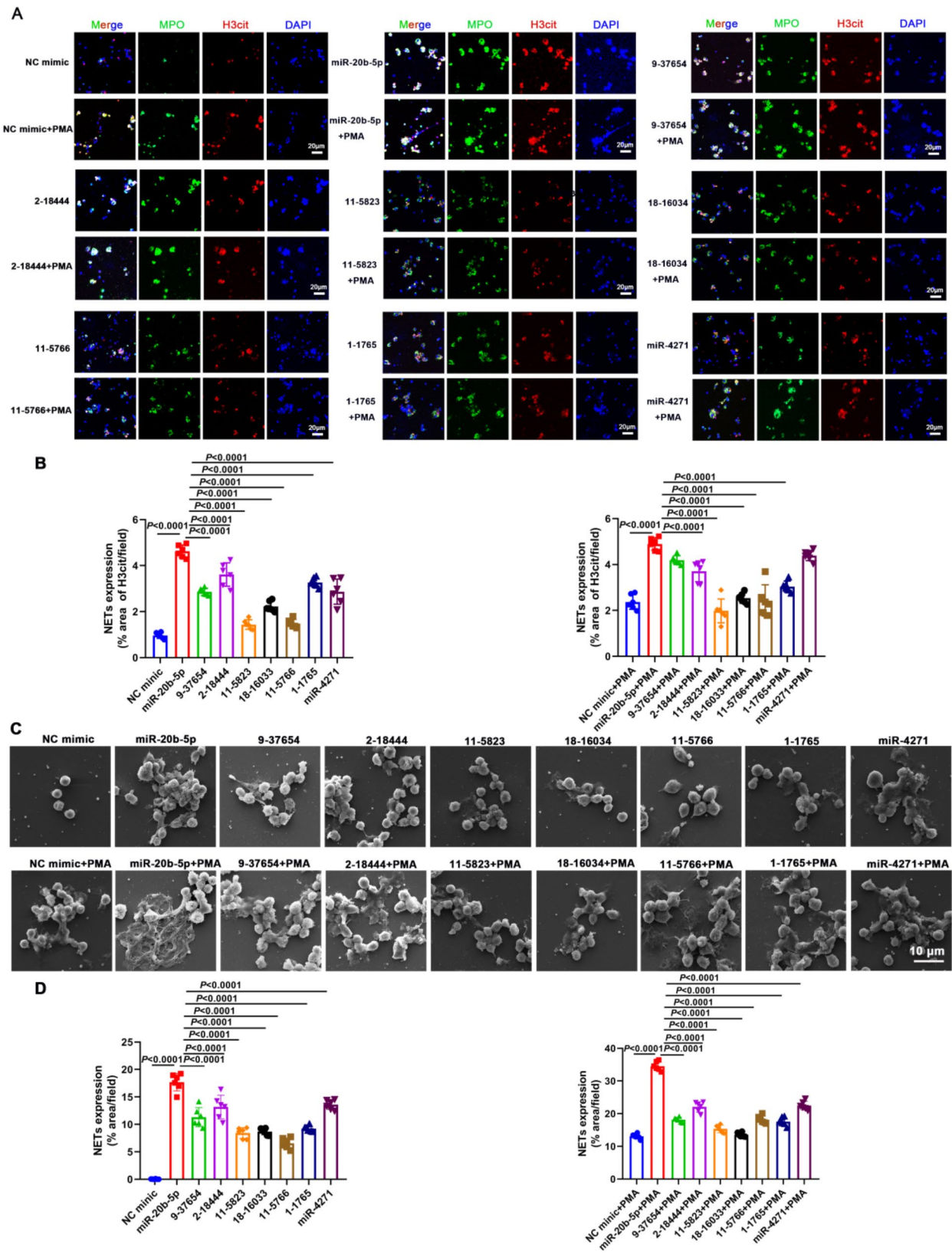
Fig. 4 (See legend on next page.)

(See figure on previous page.)

Fig. 4 Highly abundant COVID-19 patient serum-derived EVs carry specific miRNAs that are associated with NET formation. **A**-**B** Neutrophils were treated with miRNAs (miR-20b-5p, 9_37654, 2_18444, 11_5823, 18_16034, 11_5766, 1_1765, and miR-4271) and miRNAs + PMA, NETs were observed using IF (**A**) and were quantified (**B**). **C**-**D** Neutrophils were treated with miRNAs (miR-20b-5p, 9_37654, 2_18444, 11_5823, 18_16034, 11_5766, 1_1765, and miR-4271) and miRNAs + PMA, NETs were observed using SEM (**C**) and were quantified (**D**). Differences were analyzed using one-way ANOVA with Dunnett's multiple comparison test (**B** and **D**)

platelet- and granulocyte-derived EVs in patients with COVID-19 [30–33]. Consistent with these findings, our data also revealed upregulated expression of serum EVs in patients with COVID-19 compared to healthy volunteers. Previous studies have shown that COVID-19 patient plasma-derived EVs contribute to immune responses [34]. Moreover, elevated levels of TNF-α in the serum of patients with COVID-19 were found to be closely associated with the expression of CD142 expression on EVs surfaces and their procoagulant activity [35, 36]. Studies have reported a significant increase in circulating tissue factor-expressing EVs that correlated with D-dimer levels, von Willebrand factor, circulating leukocytes, and inflammatory markers. This indicates the contribution of tissue factor-expressing EVs in disease determining severity and thrombosis in patients with COVID-19 [15, 16, 31, 33]. Furthermore, EVs-derived miRNAs may also contribute to the development of thrombotic complications in patients with COVID-19 by down-regulating specific miRNAs (miR-145 and miR-885), resulting in increased levels of tissue factor and von Willebrand factor, thereby promoting a pre-thrombotic state [37]. However, the precise mechanisms by which EVs influence COVID-19 pathology, particularly thrombosis in patients, remain largely unknown. Herein, we found that COVID-19 patient serum-derived EVs are internalized by neutrophils to induce formation of NETs, which are key drivers of immunothrombosis in COVID-19 [12].

Recent studies have demonstrated that neutrophils actively participate in the formation of thrombi within blood vessels, a term called immunothrombosis [38]. NETs can also increase the size of thrombi by trapping platelets and microvesicles [39]. In addition, NETs have been shown to contribute to thrombosis in mouse models of inferior vena cava stenosis [39, 40]. Furthermore, the levels of NETs in plasma and bronchoalveolar fluid were higher in patients with transfusion-associated acute respiratory distress syndrome (ARDS) and pneumonia-associated ARDS compared to non-ARDS patients [41–43]. As a result, NETs may be promising markers of disease severity in patients with COVID-19 [21]. Elevated levels of the MPO-DNA complex, a biomarker indicating the presence of circulating NETs fragments, were observed in patients with COVID-19, especially those requiring invasive mechanical ventilation [11, 21]. In severe cases of COVID-19, neutrophils adopt a low-density phenotype that is prone to spontaneous NET formation, leading to increased intravascular aggregation,

microthrombosis, and organ damage [44]. Additionally, NETs contribute to acute lung injury by inducing macrophages to release IL-1β, which further enhances NET formation [45, 46]. Moreover, the elevated inflammatory mediators in patients with COVID-19 regulate neutrophil activity through the expression of chemotactic products [47, 48]. Herein, in this work, we show that COVID-19 patient serum-derived EVs significantly induce NET formation. This mechanism creates a self-amplifying feedback loop, resulting in exaggerated inflammatory responses and immunothrombosis in patients with COVID-19.

Importantly, miRNAs have been shown to regulate NET formation [49–51]. In this study, we observed significant differential expression of 78 miRNAs (27 up-regulated and 51 down-regulated) between the COVID-19-EVs and Normal-EVs groups. Furthermore, the results from our KEGG analysis indicate that these differentially expressed miRNAs are closely associated with NET formation. From this pool of miRNAs, we identified eight miRNAs that showed high expression levels in COVID-19-EVs, selected based on their fold changes (>180). These miRNAs were identified as 9_37654, 2_18444, 11_5823, 18_16034, 11_5766, miR-20b-5p, 1_1765, and miR-4271. Notably, all eight of these miRNAs exhibited the capability to induce NET formation. Of particular interest was the significant induction effect observed for miR-20b-5p. Previous studies have suggested that miR-20b-5p is involved in inflammation. Triptolide prevents osteoarthritis by inhibiting hsa-miR-20b [52]. The LncRNA2264/miR-20b-5p/IL17RD axis regulates hydrogen sulfide exposure-induced thymus inflammation in broilers through activation of the MYD88/NF-κB pathway [53]. Further, miR-20b promotes osteocyte apoptosis in rats with hormone-induced femoral head necrosis through BMP signaling pathway [54]. We discovered that COVID-19-EVs-mediated induction of NET formation significantly decreased upon inhibition of miR-20b-5p, thereby confirming the crucial role of miR-20b-5p in this process.

In conclusion, our study provides evidence that COVID-19 patient serum-derived EVs transfer specific miRNAs that promote NET formation. Our study enhances current understanding of the molecular mechanisms underlying exaggerated inflammatory storms and immunothrombosis in COVID-19 patients. Specifically, we have identified miR-20b-5p as a potential target for therapeutic intervention in COVID-19. Our results
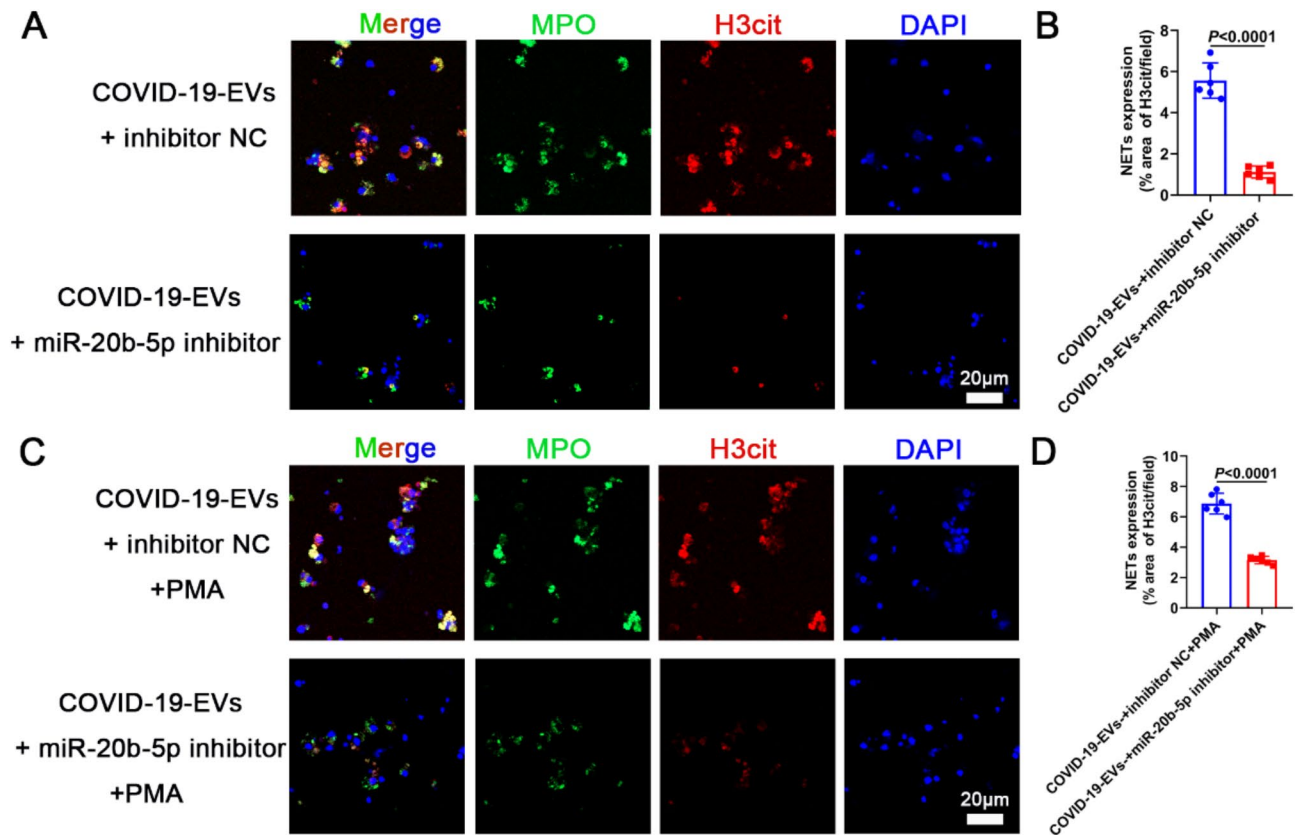
Fig. 5 COVID-19-EVs-mediated induction of NET formation decreased significantly after inhibition of miR-20b-5p. **A-B** Neutrophils were treated with COVID-19-EVs + inhibitor NC (Normal Control inhibitor) and COVID-19-EVs + miR-20b-5p inhibitor, NETs were observed using IF (**A**) and were quantified (**B**). **C-D** Neutrophils were treated with COVID-19-EVs + inhibitor NC + PMA and COVID-19-EVs + miR-20b-5p inhibitor + PMA, NETs were observed using IF (**C**) and were quantified (**D**). Differences were analyzed using unpaired two-sample *t*-test (**B** and **D**)
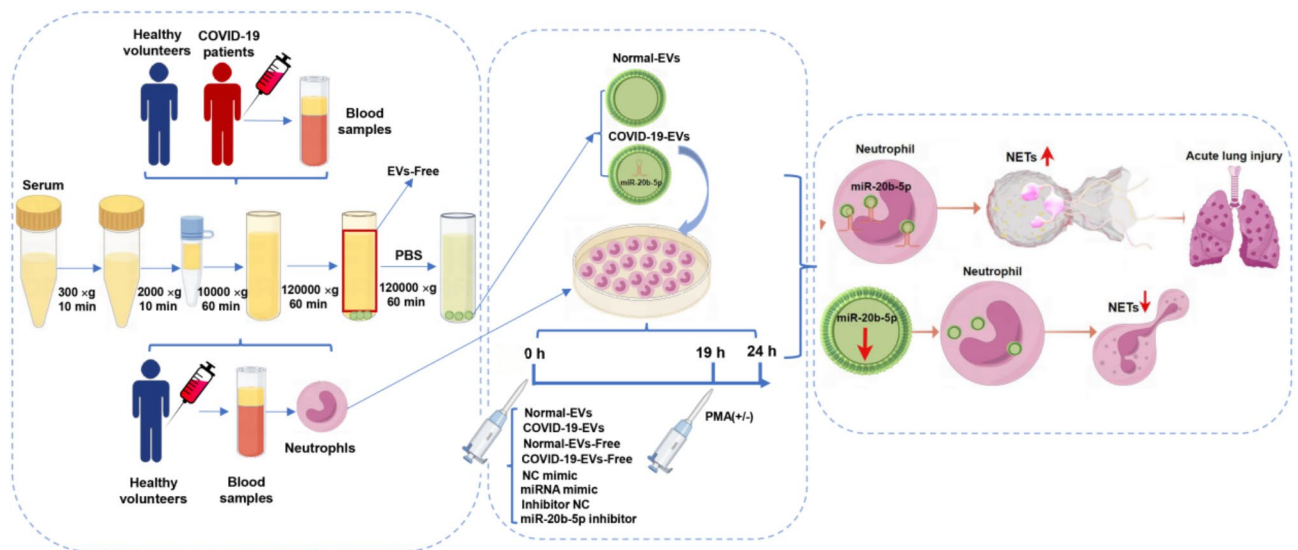
Fig. 6 COVID-19 patient serum-derived EVs deliver miR-20b-5p to induce NET formation

highlight the importance of investigating the role of EVs-derived miRNAs in the pathogenesis of COVID-19 pathogenesis and present a promising opportunity for the development of novel therapeutic strategies.

Supplementary Information

Supplementary Material 1

Supplementary Material 2

Data availability
No datasets were generated or analysed during the current study.

Declarations

Ethics approval and consent to participate
The study was approved by the ethics committee of The Second Affiliated Hospital of Guangzhou Medical University (approval number 2023-hs-17-02).

Consent for publication
Not applicable.

Competing interests
The authors declare no competing interests.

Author details
¹KingMed School of Laboratory Medicine, The Second Affiliated Hospital, The Affiliated Traditional Chinese Medicine Hospital, Guangzhou Medical University, Guangzhou 511436, China
²Department of Parasitology of Zhongshan School of Medicine, Sun Yat-sen University, Guangzhou 510080, China
³Institute of Virology, Helmholtz Centre Munich — German Research Centre for Environmental Health, 85764 Neuherberg, Germany
⁴Chair for Preventions of Infectious Microbial Diseases, School of Life Sciences, Central Institute of Disease Prevention, Technical University of Munich, 85354 Freising, Germany

References
1. Merad M, Blish CA, Sallusto F, Iwasaki A. The immunology and immunopathology of COVID-19. Science. 2022;375(6585):1122–7.
2. Schulte-Schrepping J, Reusch N, Paclik D, Baßler K, Schlickeiser S, Zhang B, et al. Severe COVID-19 is marked by a dysregulated myeloid cell compartment. Cell. 2020;182(6):1419–e4023.
3. Silvin A, Chapuis N, Dunsmore G, Goubet A-G, Dubuisson A, Derosa L, et al. Elevated calprotectin and abnormal myeloid cell subsets discriminate severe from mild COVID-19. Cell. 2020;182(6):1401–e1818.
4. Borges L, Pithon-Curi TC, Curi R, Hatanaka E. COVID-19 and neutrophils: the relationship between hyperinflammation and neutrophil extracellular traps. Mediators Inflamm. 2020;2020:8829674.
5. Lambour J, Naranjo-Gomez M, Boyer-Clavel M, Pelegrin M. Differential and sequential immunomodulatory role of neutrophils and Ly6C(hi) inflammatory monocytes during antiviral antibody therapy. Emerg Microbes Infect. 2021;10(1):964–81.
6. Wang J, Li Q, Qiu Y, Lu H. COVID-19: imbalanced cell-mediated immune response drives to immunopathology. Emerg Microbes Infect. 2022;11(1):2393–404.
7. Zhang B, Zhou X, Zhu C, Song Y, Feng F, Qiu Y, et al. Immune phenotyping based on the neutrophil-to-lymphocyte ratio and IgG level predicts disease severity and outcome for patients with COVID-19. Front Mol Biosci. 2020;7:157.
8. Shi H, Zuo Y, Yalavarthi S, Gockman K, Zuo M, Madison JA, et al. Neutrophil calprotectin identifies severe pulmonary disease in COVID-19. J Leukoc Biol. 2021;109(1):67–72.
9. Melero I, Villalba-Esparza M, Recalde-Zamacona B, Jiménez-Sánchez D, Teijeira Á, Argueta A, et al. Neutrophil extracellular traps, local IL-8 expression, and cytotoxic T-lymphocyte response in the lungs of patients with fatal COVID-19. Chest. 2022;162(5):1006–16.
10. Veras FP, Pontelli MC, Silva CM, Toller-Kawahisa JE, de Lima M, Nascimento DC, et al. SARS-CoV-2-triggered neutrophil extracellular traps mediate COVID-19 pathology. J Exp Med. 2020;217(12):e20201129.
11. Zuo Y, Yalavarthi S, Shi H, Gockman K, Zuo M, Madison JA, et al. Neutrophil extracellular traps in COVID-19. JCI Insight. 2020;5(11):e138999.
12. Skendros P, Mitsios A, Chrysanthopoulou A, Mastellos DC, Metallidis S, Rafailidis P, et al. Complement and tissue factor-enriched neutrophil extracellular traps are key drivers in COVID-19 immunothrombosis. J Clin Invest. 2020;130(11):6151–7.
13. Caillon A, Trimaille A, Favre J, Jesel L, Morel O, Kauffenstein G. Role of neutrophils, platelets, and extracellular vesicles and their interactions in COVID-19-associated thrombopathy. J Thromb Haemost. 2022;20(1):17–31.
14. Ebeyer-Masotta M, Eichhorn T, Weiss R, Lauková L, Weber V. Activated platelets and platelet-derived extracellular vesicles mediate COVID-19-associated immunothrombosis. Front Cell Dev Biol. 2022;10:914891.
15. Guervilly C, Bonifay A, Burtey S, Sabatier F, Cauchois R, Abdili E, et al. Dissemination of extreme levels of extracellular vesicles: tissue factor activity in patients with severe COVID-19. Blood Adv. 2021;5(3):628–34.
16. Rosell A, Havervall S, von Meijenfeldt F, Hisada Y, Aguilera K, Grover SP, et al. Patients with COVID-19 have elevated levels of circulating extracellular vesicle tissue factor activity that is associated with severity and mortality-brief report. Arterioscler Thromb Vasc Biol. 2021;41(2):878–82.
17. Garcia-Martin R, Wang G, Brandão BB, Zanotto TM, Shah S, Kumar Patel S, et al. MicroRNA sequence codes for small extracellular vesicle release and cellular retention. Nature. 2022;601(7893):446–51.
18. Yang L, Liu Q, Zhang X, Liu X, Zhou B, Chen J, et al. DNA of neutrophil extracellular traps promotes cancer metastasis via CCDC25. Nature. 2020;583(7814):133–8.
19. Wang L, Liao Y, Yang R, Yu Z, Zhang L, Zhu Z, et al. Sja-miR-71a in Schistosome egg-derived extracellular vesicles suppresses liver fibrosis caused by schistosomiasis via targeting semaphorin 4D. J Extracell Vesicles. 2020;9(1):1785738.
20. Maxwell AJ, Ding J, You Y, Dong Z, Chehade H, Alvero A, et al. Identification of key signaling pathways induced by SARS-CoV2 that underlie thrombosis and vascular injury in COVID-19 patients. J Leukoc Biol. 2021;109(1):35–47.
21. Middleton EA, He X-Y, Denorme F, Campbell RA, Ng D, Salvatore SP, et al. Neutrophil extracellular traps contribute to immunothrombosis in COVID-19 acute respiratory distress syndrome. Blood. 2020;136(10):1169–79.
22. Sollberger G, Choidas A, Burn GL, Habenberger P, Di Lucrezia R, Kordes S, et al. Gasdermin D plays a vital role in the generation of neutrophil extracellular traps. Sci Immunol. 2018;3(26):eaar6689.

23. Mori MA, Ludwig RG, Garcia-Martin R, Brandão BB, Kahn CR. Extracellular miRNAs: from biomarkers to mediators of physiology and disease. Cell Metab. 2019;30(4):656–73.

24. Bonnet CS, Williams AS, Gilbert SJ, Harvey AK, Evans BA, Mason DJ. AMPA/kainate glutamate receptors contribute to inflammation, degeneration and pain related behaviour in inflammatory stages of arthritis. Ann Rheum Dis. 2015;74(1):242–51.

25. Jiao Y, Li W, Wang W, Tong X, Xia R, Fan J, et al. Platelet-derived exosomes promote neutrophil extracellular trap formation during septic shock. Crit Care. 2020;24(1):380.

26. Futosi K, Fodor S, Mócsai A. Reprint of Neutrophil cell surface receptors and their intracellular signal transduction pathways. Int Immunopharmacol. 2013;17(4):1185–97.

27. Bando K, Kuroishi T, Tada H, Oizumi T, Tanaka Y, Takahashi T, et al. Nitrogen-containing bisphosphonates and lipopolysaccharide mutually augment inflammation via adenosine triphosphate (ATP)-mediated and interleukin 1β (IL-1β)-mediated production of neutrophil extracellular traps (NETs). J Bone Min Res. 2021;36(9):1866–78.

28. Gao T, Li J, Shi L, Hu B. Rosavin inhibits neutrophil extracellular traps formation to ameliorate sepsis-induced lung injury by regulating the MAPK pathway. Allergol Immunopathol (Madr). 2023;51(4):46–54.

29. Domingo-Gonzalez R, Martínez-Colón GJ, Smith AJ, Smith CK, Ballinger MN, Xia M, et al. Inhibition of neutrophil extracellular trap formation after stem cell transplant by prostaglandin E2. Am J Respir Crit Care Med. 2016;193(2):186–97.

30. Zaid Y, Puhm F, Allaeys I, Naya A, Oudghiri M, Khalki L, et al. Platelets can associate with SARS-Cov-2 RNA and are hyperactivated in COVID-19. Circ Res. 2020;127(11):1404–18.

31. Canzano P, Brambilla M, Porro B, Cosentino N, Tortorici E, Vicini S, et al. Platelet and endothelial activation as potential mechanisms behind the thrombotic complications of COVID-19 patients. JACC Basic Transl Sci. 2021;6(3):202–18.

32. Taus F, Salvagno G, Canè S, Fava C, Mazzaferri F, Carrara E, et al. Platelets promote thromboinflammation in SARS-CoV-2 pneumonia. Arterioscler Thromb Vasc Biol. 2020;40(12):2975–89.

33. Krishnamachary B, Cook C, Kumar A, Spikes L, Chalise P, Dhillon NK. Extracellular vesicle-mediated endothelial apoptosis and EV-associated proteins correlate with COVID-19 disease severity. J Extracell Vesicles. 2021;10(9):e12117.

34. Pesce E, Manfrini N, Cordiglieri C, Santi S, Bandera A, Gobbini A, et al. Exosomes recovered from the plasma of COVID-19 patients expose SARS-CoV-2 spike-derived fragments and contribute to the adaptive immune response. Front Immunol. 2021;12:785941.

35. Balbi C, Burrello J, Bolis S, Lazzarini E, Biemmi V, Pianezzi E, et al. Circulating extracellular vesicles are endowed with enhanced procoagulant activity in SARS-CoV-2 infection. EBioMedicine. 2021;67:103369.

36. Mackman N, Grover SP, Antoniak S. Tissue factor expression, extracellular vesicles, and thrombosis after infection with the respiratory viruses influenza a virus and coronavirus. J Thromb Haemost. 2021;19(11):2652–8.

37. Gambardella J, Kansakar U, Sardu C, Messina V, Jankauskas SS, Marfella R, et al. Exosomal miR-145 and miR-885 regulate thrombosis in COVID-19. J Pharmacol Exp Ther. 2023;384(1):109–15.

38. Engelmann B, Massberg S. Thrombosis as an intravascular effector of innate immunity. Nat Rev Immunol. 2013;13(1):34–45.

39. Budnik I, Brill A. Immune factors in deep vein thrombosis initiation. Trends Immunol. 2018;39(8):610–23.

40. Martinod K, Wagner DD. Thrombosis: tangled up in NETs. Blood. 2014;123(18):2768–76.

41. Rebetz J, Semple JW, Kapur R. The pathogenic involvement of neutrophils in acute respiratory distress syndrome and transfusion-related acute lung injury. Transfus Med Hemother. 2018;45(5):290–8.

42. Bendib I, de Chaisemartin L, Granger V, Schlemmer F, Maitre B, Hüe S, et al. Neutrophil extracellular traps are elevated in patients with pneumonia-related acute respiratory distress syndrome. Anesthesiology. 2019;130(4):581–91.

43. Lv X, Wen T, Song J, Xie D, Wu L, Jiang X, et al. Extracellular histones are clinically relevant mediators in the pathogenesis of acute respiratory distress syndrome. Respir Res. 2017;18(1):165.

44. Leppkes M, Knopf J, Naschberger E, Lindemann A, Singh J, Herrmann I, et al. Vascular occlusion by neutrophil extracellular traps in COVID-19. EBioMedicine. 2020;58:102925.

45. Channappanavar R, Perlman S. Pathogenic human coronavirus infections: causes and consequences of cytokine storm and immunopathology. Semin Immunopathol. 2017;39(5):529–39.

46. Chousterman BG, Swirski FK, Weber GF. Cytokine storm and sepsis disease pathogenesis. Semin Immunopathol. 2017;39(5):517–28.

47. Huang C, Wang Y, Li X, Ren L, Zhao J, Hu Y, et al. Clinical features of patients infected with 2019 novel coronavirus in Wuhan, China. Lancet. 2020;395(10223):497–506.

48. Bösmüller H, Traxler S, Bitzer M, Häberle H, Raiser W, Nann D, et al. The evolution of pulmonary pathology in fatal COVID-19 disease: an autopsy study with clinical correlation. Virchows Arch. 2020;477(3):349–57.

49. Hawez A, Al-Haidari A, Madhi R, Rahman M, Thorlacius H. MiR-155 regulates PAD4-dependent formation of neutrophil extracellular traps. Front Immunol. 2019;10:2462.

50. Arroyo AB, de Los Reyes-García AM, Rivera-Caravaca JM, Valledor P, García-Barberá N, Roldán V, et al. MiR-146a regulates neutrophil extracellular trap formation that predicts adverse cardiovascular events in patients with atrial fibrillation. Arterioscler Thromb Vasc Biol. 2018;38(4):892–902.

51. Hsieh Y-T, Chou Y-C, Kuo P-Y, Tsai H-W, Yen Y-T, Shiau A-L, et al. Down-regulated miR-146a expression with increased neutrophil extracellular traps and apoptosis formation in autoimmune-mediated diffuse alveolar hemorrhage. J Biomed Sci. 2022;29(1):62.

52. Qian K, Zhang L, Shi K. Triptolide prevents osteoarthritis via inhibiting hsa-miR-20b. Inflammopharmacology. 2019;27(1):109–19.

53. Wang Y, He Y, Hu X, Chi Q, Zhao B, Ye J, et al. Regulating of LncRNA2264/miR-20b-5p/IL17RD axis on hydrogen sulfide exposure-induced inflammation in broiler thymus by activating MYD88/NF-κB pathway. Toxicology. 2022;467:153086.

54. Li GQ, Wang ZY. MiR-20b promotes osteocyte apoptosis in rats with steroid-induced necrosis of the femoral head through BMP signaling pathway. Eur Rev Med Pharmacol Sci. 2019;23(11):4599–608.

Publisher's note